Polytechnica (2024) 7:9
https://doi.org/10.1007/s41050-024-00052-4

ORIGINAL ARTICLE

Environmental Radioactivity Monitoring and Radiological Impact Assessment of Agbara Industrial Area, Ogun State, Nigeria

Mojisola Rachael Usikalu[1] · Muyiwa Michael Orosun[2] · Akinpelu Akinwumi[1] · Idowu Olaegbe Babarimisa[1] · Theophilus Emuobor Arijaje[1] · Adamu Usman Mohammed[3]

Received: 11 September 2023 / Revised: 18 September 2024 / Accepted: 19 September 2024

Abstract
This study assessed the naturally occurring radioactivity of ^{40}K, ^{238}U, and ^{232}Th, which pose a significant threat to human health, particularly when their concentrations exceed the threshold. Background radiation levels were measured at two specific locations, Access Bank and Market areas, across a total of forty (40) sample points. The measurements were taken using a calibrated RS125 Gamma Spectrometer (a portable NaI [Tl] detector) designed in Canada, in conjunction with a global positioning system (GPS) to accurately record the research coordinates within the Agbara industrial area, Ogun State, Nigeria. The mean activity concentrations of the primordial radionuclides were 177.87 Bqkg-1, 20.01 Bqkg-1, and 52.90 Bqkg-1 for ^{40}K, ^{238}U, and ^{232}Th, respectively. More so, the in-situ measured dose rate (DR) ranges between 12.18 nGyh-1 (Access Bank area) and 97.95 nGyh-1 (Market area), with an average value of 47.22 nGyh-1. The average measured and estimated absorbed dose rates were within the safe limit of 57 nGyh-1 provided by UNSCEAR. However, the measured dose rates exceeded the recommended limit in ten locations, while measured activity for thorium exceeded the world average value for over half of the study locations. Although all estimated radiological parameters were within recommended threshold values, suggesting the low risk of exposure to higher levels of ionising radiation in most locations in the Agbara industrial area, there is a potential cancer risk for individuals who have resided in the area for 70 years or more due to long-term exposure to ionising radiation.

Keywords Radioactivity · Radiation hazards · Environmental assessment impact · Agbara industrial estate · Ogun state

1 Introduction

The ubiquitous presence of naturally occurring terrestrial radionuclides permeates every stratum of the Earth's ecosystem, resulting in incessant exposure of human populations to ionizing radiation. Prolonged exposure to ionizing radiation poses significant health risks, including carcinogenesis and induction of radiation-induced pathologies (Omeje et al. 2024; UNSCEAR, 2008). Consequently, vigilant monitoring of environmental radioactivity is imperative to mitigate exposure levels beyond the established threshold limits.

The resultant data from these monitoring efforts provide invaluable insights into the spatial distribution and activity concentrations of primordial radionuclides, including the 238U and 234Th decay series, as well as the non-series radionuclide 40 K. This information is crucial for assessing radiation exposure risks and informing evidence-based strategies for radiation protection and environmental remediation. This result of the environmental radioactivity study can serve as an important radiological baseline submission by establishing the current levels of naturally occurring radionuclides in Agbara areas, allowing for the proper identification of any increases in radiation levels over time, particularly in areas affected by industrial activities. Also, it will make it easier to assess the potential health risks to the local population with the intention of formulating effective strategies for adverse health effects reduction, as well

✉ Muyiwa Michael Orosun
r466@ipc.fukushima-u.ac.jp

[1] Department of Physics, Covenant University, Ota, Nigeria

[2] Institute of Environmental Radioactivity, Fukushima University, Fukushima city, Japan

[3] Department of Applied Geology, Abubakar Tafawa Balewa University, Bauchi, Nigeria

Published online: 01 October 2024

as instituting remediation steps and enacting radiation protection laws. (Usikalu et al. 2020; Omeje et al. 2021, 2022; Ajibola et al. 2022). The level of background radioactivity has been reported to be elevated by anthropogenic activities such as mining (Orosun et al. 2021, 2022a, b), Agricultural activities (Orosun et al. 2017), industrial activities such as the ones at Agbara industrial areas (Usikalu et al. 2020) or geogenic processes (Orosun et al. 2020).

In Nigeria, many works have been carried out on environmental radioactivity from different areas of the country (Adagunoado et al., 2019; Adagunodo et al. 2018; Ademola et al. 2014; Usikalu et al. 2016, 2017; Orosun et al. 2022a). This study is intended to supplement and broaden the existing data on radiological impact assessment in the country with specific interest in the Agbara industrial areas, Ogun State. This is necessary because it provides needed baseline information on the level of radiation exposures in the industrial areas as benchmark for future reference on the radiological health impacts on the residents of the study areas. It also address the SDG goal 3 as it relates to the good health and well-being of those in the study area.

2 Materials and Methods

2.1 Study Area

Agbara Industrial area is one of the largest industrial estates in sub-Saharan Africa. The industrial area is a model integrated Town development on 454.1 hectares of land. It is situated approximately 31 km west of Lagos on the Lagos-Badagry expressway on high ground above the Owo River and derives its name from the neighbouring Agbara village. It center lies at 6°31′0″ North, 3°6′0″ East (www.gomapper.com) and it has an elevation of 37 m above sea level. The industrial areas are made up of 41.55% (188.289 hectares) of the whole estate. The location and accessibility of Agbara Estate makes the transportation of raw materials and finished goods informed the location as a good industrial area. Figure 1 shows the map of the study area. The geology of Ota is generally made up of sedimentary rocks of the Dahomey Basin (Fig. 1). The lithostratigraphy sequences underlying the study area are Abeokuta, Ewekoro, Oshosun, Ilaro, and Benin Formations. Recently, an Alluvium which are of sands and shales are considered as the youngest of all these sequences, while Abeokuta Formation is considered as the oldest (Adagunoado et al., 2019; Adagunodo et al. 2018). As revealed in Fig. 1, the study area falls on the Benin Formation, which is known as Coastal Plain Sands. This sequence is of Pliocene age, which is majorly composed of continental sands and intercalations of clay and shale within these sands (Usikalu et al. 2020).

2.2 In-Situ Radioactivity Measurements Using Super-Spec RS125 Gamma Spectrometer

To accurately assess the radiological characteristics of the study locations, a handheld RS-125 gamma ray spectrometer, manufactured by the Canadian Geophysical Institute, Canada, was employed. This state-of-the-art instrument features a 2.0 × 2.0 NaI(Tl) crystal detector, providing a wide energy range of 30–3000 keV for detecting terrestrial radiation (Usikalu et al. 2023). The spectrometer was calibrated using 1 × 1 m test pads, accumulating spectra for 5 min for Uranium, Thorium, and Potassium, and 10 min for terrestrial pads. This rigorous calibration process ensured optimal accuracy and precision (Omeje et al. 2023).

To ensure spatial accuracy, a global positioning system (GPS) was utilized to record the coordinates of each sampling point. A total of 20 sampling points were surveyed, with repeated measurements taken at each location to account for any variability. The mean values of these measurements were subsequently calculated for data analysis. The RS-125 spectrometer's robust design, high precision, and user-friendly interface make it an ideal tool for geophysical assessments. Its extensive data storage capacity allows for the collection of multiple readings, facilitating comprehensive radiological surveys. The measured parameters included: Absorbed dose rate and the activity concentration of ^{40}K, ^{238}U, and ^{232}Th. This integrated approach enabled a thorough characterization of the radiological environment at the study locations, providing valuable insights for future research and environmental monitoring initiatives. The activity concentration of the measured radionuclides was taken in part per million (ppm) for ^{238}U, ^{232}Th and percentage (%) for ^{40}K. The measured values were converted to Becquerel per kilograms (Bq/kg) using the conversion factor reported by (IAEA 1989; Oyeyemi et al. 2017; Usikalu et al. 2023).

2.3 Evaluation of the In-Situ Radiological Hazard Indices

The absorbed dose rate assesses the effects of exposure to ionizing radiation on living cells. This was evaluated using Eq. (1)

$$D\,(nGyh^{-1}) = 0.462K_U + 0.604K_{Th} + 0.0416K_K \quad (1)$$

D *(nGyh^{-1})* is the dose rate, K_U,K_{Th}, K_K are the activity concentration of ^{238}U, ^{232}Th, and ^{40}K in Bqkg^{-1} respectively (UNSCEAR, 2000).

The Annual effective dose equivalent (AEDE) is the effective dose over a period of a year. This was obtained using Eq. (2).

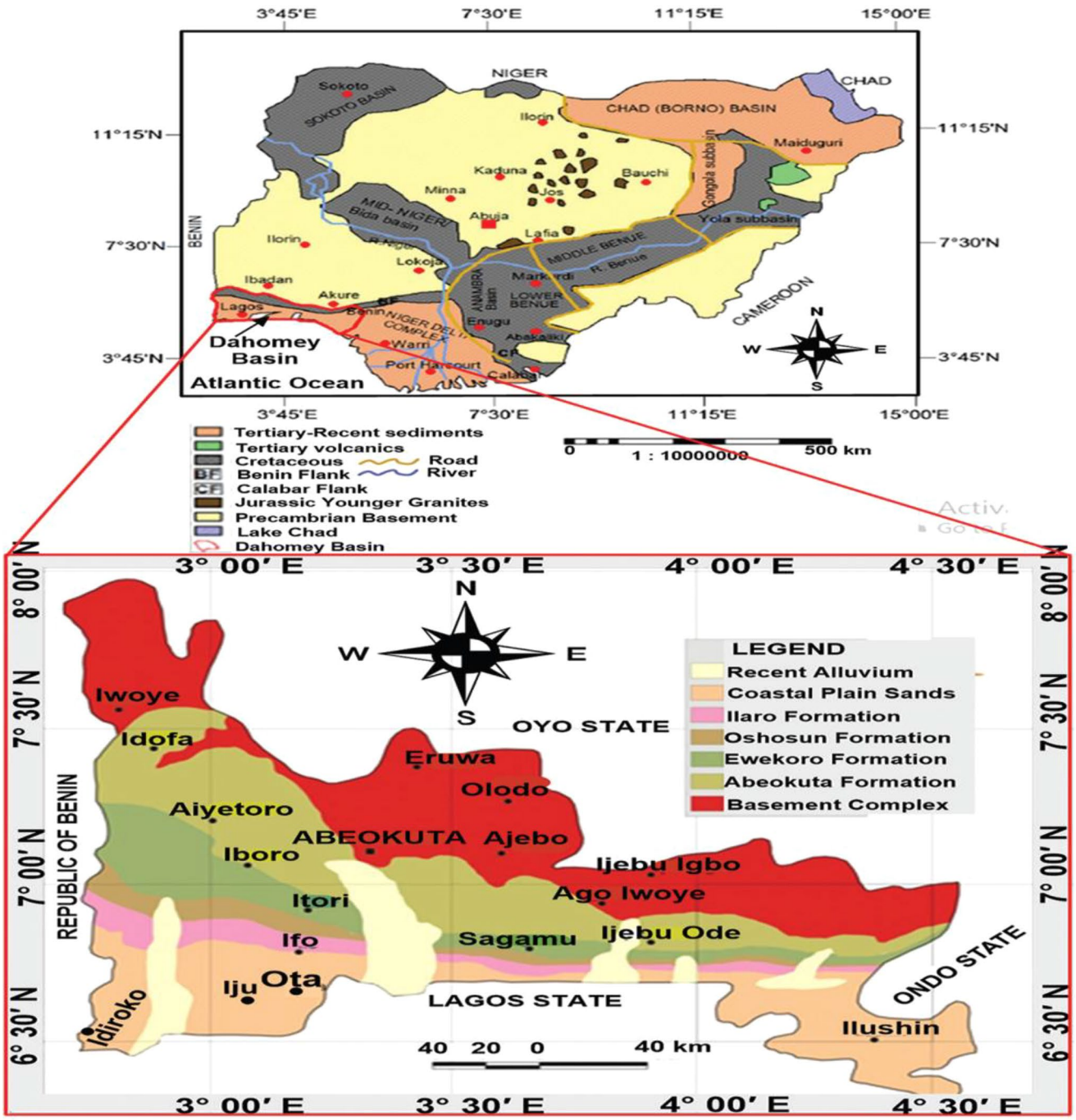

Fig. 1 Geological map of ogun state. source: (Usikalu et al. 2020)

$$AEDE = D \times O_F \times C_C \times 8760 \quad (2)$$

$$ELCR = AEDE \times DL \times RF \quad (3)$$

D represent the absorbed dose, O_F is the occupancy factor that was taken as 0.2 for outdoor and 0.8 for indoor, C_C represents the conversion coefficient which was be taken as 0.7 (UNSCEAR, 2000).

The excess lifetime cancer risk measures the probability of the risk of cancer disease to the dweller around the market, was obtained using the Eq. (3)

AEDE is the annual equivalent dose, *DL* is the average duration of life which was taken as 65 years and *RF* is the risk factor (Sv^{-1}) was taken as 0.05 (UNSCEAR, 2000).

The external hazard index measure the radiation risk as a result of external exposure in the study area, while the internal hazard index estimates the hazard to the respiratory organs from internal exposure to radon and its progeny. The

external hazard index and the internal hazard index were estimated using Eqs. (4 and 5).

$$H_{ext} = \frac{K_U}{370} + \frac{K_{Th}}{259} + \frac{K_K}{4810} \tag{4}$$

$$H_{int} = \frac{K_U}{185}\frac{K_{Th}}{259}\frac{K_K}{4810} \tag{5}$$

Radium equivalent activity Raeq (Bq/kg) assesses the gamma output from different mixture of ^{238}U, ^{232}Th, ^{40}K in an environment. It was estimated using Eq. (6) (UNSCEAR, 2000).

$$Ra_{eq} = K_U + 1.43K_{Th} + 0.077K_k \tag{6}$$

Gamma representative index measure the gamma radiation hazard due to the natural radionuclides in the particular material being assessed. This was calculated using Eq. (7) (UNSCEAR, 2000).

$$I_Y = \frac{K_U}{150} + \frac{K_{Th}}{100} + \frac{K_K}{1500} \tag{7}$$

3 Results and Discussion

3.1 In-Situ Activity Concentration Using Handheld Super-Spec RS125

The mean in situ measured activity concentrations of ^{238}U, ^{232}Th, ^{40}K and the gamma dose rate (*DR*) is provided in Table 1. The descriptive statistics for the in-situ measured activity concentrations and the gamma dose rate (*DR*) measured in Table 1 were estimated using Microsoft Excel, which makes it easy to draw scientific clarifications on the data as presented in Table 2. More so, the coordinates obtained through the Global Positioning System (GPS) at the research locations were used to create visual representations of the concerned radionuclide concentrations (^{40}K, ^{238}U, ^{232}Th, and dose rates) distributions using the interpolation technique through GIS software as presented in Figs. 2, 3, 4 and 5. The results revealed that the activity concentration of ^{238}U and ^{232}Th, were slightly skewed (having almost a symmetric distribution) since most of the measure of the asymmetry of their probability distribution about their means falls outside the range of -1 and +1. While ^{40}K and the gamma dose rate (DR) whose skew values falls within the range of -1 and +1, were normally distributed (Orosun et al. 2019).

From Table 2, the lowest mean values of the activity concentration of ^{40}K, ^{238}U, ^{232}Th and the gamma dose-rate are below the detection limit (AG23, Mentos area); (AG31, Access bank area); (AG23, Mentos area) $Bqkg^{-1}$ and 12.18 $nGyh^{-1}$ (AG31, Access Bank Area) respectively. While their corresponding highest values are 472.14 $Bqkg^{-1}$ (Access bank area), 72.88 $Bqkg^{-1}$ (AG7, Market area), 148.00 $Bqkg^{-1}$ (AG40, Agbara bus stop) and 97.95 $nGyh^{-1}$ (Market), respectively. These high and low values of the activity concentration of ^{40}K, ^{238}U, ^{232}Th and the gamma dose-rate were revealed by the spatial distribution map (Figs. 2, 3, 4 and 5). The highest values obtained for the concentrations of ^{238}U, ^{232}Th, ^{40}K, and the gamma dose rate (*DR*) exceeds their corresponding global average values in 7 (17.50%), 23 (57.50%), 1 (2.50%) and 10 (25.00%) of the locations respectively.

The estimated overall mean values for the in-situ measured activity concentrations of ^{238}U, ^{232}Th, ^{40}K, and the gamma dose rate (*DR*) are 20.01 $Bqkg^{-1}$, 52.90 $Bqkg^{-1}$, 177.87 $Bqkg^{-1}$, and 47.22 $nGyh^{-1}$, respectively. The overall mean values of the activity concentration of the radionuclides are below 32.00, 420.00 $Bqkg^{-1}$ and 59.00 $nGyh^{-1}$ global average values for exposure to ^{238}U, ^{40}K, and the gamma dose rate (*DR*) respectively, provided by ICRP (1991), IAEA (1996) and UNSCEAR (2000). Only the mean value of ^{232}Th (52.90 $Bqkg^{-1}$) exceeds its global average value of 45.00 $Bqkg^{-1}$.

Pearson correlation analysis was carried out to further investigate the connection between these measured radionuclides and the in-situ measured outdoor gamma dose rate. The result of the correlation analysis, which is presented in Table 3, were classified according to the correlation coefficient R (Orosun et al. 2019, 2020) i.e.

$0.7 \leq |R| \leq 1$ indicates a strong correlation;
$0.5 \leq |R| \leq 0.7$ suggests a significant correlation;
$0.3 \leq |R| \leq 0.5$ reveals a weak correlation; and.
$|R| < 0.3$ indicates an insignificant correlation.

A significant correlation exists between DR and ^{232}Th ($R = 0.60$) as well as between DR and ^{40}K ($R = 0.50$) and between ^{40}K and ^{232}Th ($R = 0.57$). A weak correlation was found to exist between DR and ^{238}U ($R = 0.30$). However, a negative but insignificant correlation was observed between ^{40}K and ^{238}U (R = -0.02), between ^{238}U and ^{232}Th (R = -0.12). The correlation results confirm that the enhanced outdoor dose rates at the locations was caused largely by ^{232}Th, followed by ^{40}K and then ^{238}U as shown in Table 3.

Table 1 Mean in-situ measured activities of ^{40}K, ^{238}U, ^{232}Th and the gamma dose-rate (DR) in all the locations in Agbara

S/*N*	Location	Latitude	Longitude	DR ($nGyh^{-1}$)	^{40}K ($Bqkg^{-1}$)	^{238}U ($Bqkg^{-1}$)	^{232}Th ($Bqkg^{-1}$)
1	AG1	6.504708	3.089176	12.85 ± 0.90	0.77 ± 1.55	27.37 ± 2.10	1.23 ± 0.89
2	AG2	6.500614	3.086086	25.80 ± 2.20	47.99 ± 40.88	30.14 ± 20.52	22.65 ± 16.00
3	AG3	6.507735	3.088832	56.33 ± 5.70	143.19 ± 42.63	16.61 ± 12.16	79.64 ± 14.15
4	AG4	6.499700	3.092300	37.10 ± 0.22	77.40 ± 39.97	14.15 ± 1.59	41.31 ± 2.75
5	AG5	6.503389	3.097072	44.75 ± 2.35	296.44 ± 39.03	5.54 ± 1.59	44.49 ± 1.27
6	AG6	6.487200	2.990300	50.20 ± 20.23	123.84 ± 91.14	44.588 ± 16.79	46.13 ± 32.30
7	AG7	6.513678	3.092952	88.73 ± 1.75	290.25 ± 203.56	72.878 ± 23.17	70.93 ± 4.91
8	AG8	6.500350	3.088866	50.18 ± 3.12	317.34 ± 15.48	19.07 ± 7.94	45.92 ± 0.75
9	AG9	6.506515	3.090206	40.58 ± 3.62	77.40 ± 64.45	30.44 ± 7.87	44.18 ± 6.62
10	AG10	6.504600	3.094300	30.75 ± 1.65	301.09 ± 38.78	1.85 ± 1.59	23.58 ± 2.65
11	AG11	6.504021	3.100375	77.78 ± 3.80	402.48 ± 97.90	32.90 ± 4.96	67.86 ± 8.42
12	AG12	6.501131	3.086429	30.08 ± 1.20	77.40 ± 39.97	13.22 ± 6.69	29.21 ± 3.87
13	AG13	6.487200	2.990300	38.75 ± 5.84	139.32 ± 39.97	0.62 ± 0.71	51.35 ± 6.46
14	AG14	6.516681	3.075786	34.15 ± 2.21	77.40 ± 17.87	25.83 ± 2.46	27.88 ± 3.46
15	AG15	6.510900	3.123900	50.70 ± 8.89	278.64 ± 66.88	13.22 ± 4.75	50.53 ± 13.43
16	AG16	6.514377	3.073164	60.25 ± 1.63	178.02 ± 15.48	11.59 ± 10.97	70.62 ± 11.87
17	AG17	6.847200	2.990300	42.16 ± 9.62	281.22 ± 100.19	11.38 ± 9.60	60.95 ± 14.42
18	AG18	6.512485	3.079906	90.13 ± 6.85	278.64 ± 211.50	61.19 ± 36.41	86.92 ± 17.47
19	AG19	6.464795	3.180979	67.78 ± 3.99	270.90 ± 58.61	12.92 ± 8.37	70.10 ± 9.10
20	AG20	6.501910	3.098582	97.95 ± 3.85	356.04 ± 17.87	22.76 ± 9.29	98.91 ± 8.18
21	AG21	6.589900	3.087100	38.33 ± 19.15	185.76 ± 151.67	43.36 ± 20.32	49.71 ± 5.63
22	AG22	6.512996	3.092952	55.05 ± 5.04	201.24 ± 39.97	20.91 ± 12.58	56.17 ± 6.11
23	AG23	6.504700	3.094300	18.74 ± 1.00	BDL	45.51 ± 1.42	BDL
24	AG24	6.505833	3.095012	40.99 ± 13.43	201.24 ± 156.85	34.13 ± 13.64	34.13 ± 22.93
25	AG25	6.503339	3.094882	32.35 ± 1.44	135.45 ± 14.82	14.76 ± 10.58	32.49 ± 8.87
26	AG26	6.495087	3.136347	37.13 ± 1.38	135.45 ± 34.32	4.00 ± 2.91	45.20 ± 6.08
27	AG27	6.504700	3.094300	29.20 ± 3.34	99.85 ± 16.46	11.22 ± 9.15	31.88 ± 0.39
28	AG28	6.515619	3.076343	25.25 ± 0.21	51.86 ± 14.60	5.04 ± 3.63	29.32 ± 2.38
29	AG29	6.511589	3.076129	46.53 ± 1.52	193.50 ± 92.45	18.76 ± 4.75	46.64 ± 1.08
30	AG30	6.504900	3.943000	71.33 ± 13.94	263.16 ± 96.26	16.61 ± 9.76	83.33 ± 15.94
31	AG31	6.500558	3.092266	12.18 ± 1.66	472.14 ± 108.36	BDL	118.29 ± 13.30
32	AG32	6.503389	3.092266	43.88 ± 1.62	185.76 ± 25.28	17.22 ± 12.42	41.31 ± 5.54
33	AG33	6.504071	3.086086	35.60 ± 2.60	62.69 ± 1.55	17.84 ± 4.20	35.77 ± 4.94
34	AG34	6.501683	3.095356	37.05 ± 4.78	34.83 ± 26.44	21.83 ± 13.19	34.34 ± 3.87
35	AG35	6.503457	3.095993	27.40 ± 1.16	44.89 ± 30.07	13.22 ± 1.18	32.19 ± 1.59
36	AG36	6.496429	3.084797	59.75 ± 1.35	139.32 ± 39.97	5.84 ± 1.18	75.34 ± 3.32
37	AG37	6.504600	3.094300	57.45 ± 0.39	208.21 ± 33.48	0.00 ± 0.00	63.35 ± 1.52
38	AG38	6.511465	3.099994	55.25 ± 2.22	181.89 ± 31.91	28.91 ± 10.56	55.00 ± 2.76
39	AG39	6.498057	3.088499	79.20 ± 9.77	170.28 ± 73.70	7.07 ± 2.54	69.19 ± 4.89
40	AG40	6.496911	3.086679	59.28 ± 3.33	131.58 ± 52.87	5.84 ± 1.18	148.01 ± 6.19
	Global Average (UNSCEAR, 2000)			59.00	450.00	32.00	45.00

BDL means below detection limit

Table 2 Descriptive statistics of the in-situ measured activities of ^{40}K, ^{238}U, ^{232}Th and the gamma dose-rate (DR) of all the locations in Agbara

Stat	DR ($nGyh^{-1}$)	^{40}K ($Bqkg^{-1}$)	^{238}U ($Bqkg^{-1}$)	^{232}Th ($Bqkg^{-1}$)
Minimum	12.18	0.00	0.00	0.00
Maximum	97.95	472.14	72.88	148.00
Mean	47.22	177.87	20.01	52.90
Standard Error	3.25	17.65	2.57	4.55
Median	43.02	174.15	16.61	46.38
Standard Dev	20.55	111.62	16.27	28.75
Sample Variance	422.27	12460.14	264.71	826.44
Kurtosis	0.12	-0.09	2.19	2.29
Skewness	0.66	0.53	1.37	1.05

3.2 Evaluation of the In-Situ Radiological Hazard Indices for the Selected Locations

The radiological hazard indices were estimated in order to evaluate the radiological risks for the locations. The hazards parameters calculated are presented in Table 4 and their corresponding descriptive statistics are provided in Table 5. While the outdoor absorbed dose (D_{out}) rate was obtained using Eq. 1, the in-situ measured outdoor dose rate was used to evaluate the annual effective dose equivalent (AEDE) using Eq. 2. The ensuing AEDE was eventually used for the evaluation of the excess lifetime cancer risk (ELCR) using Eq. 3.

The maximum and minimum values of the evaluated outdoor absorbed dose rate are 97.56 and 13.42 $nGyh^{-1}$, with an overall mean of 48.59 $nGyh^{-1}$. The maximum and minimum values of the AEDE were observed in the Agbara Bustop (AG40) with 0.12 $mSvy^{-1}$ and Milo area (AG1) with 0.02 $mSvy^{-1}$, respectively. Expectedly, this AG40 corresponds to the location of high activity concentration of value of ^{232}Th (i.e. 148.01 ± 6.19 $Bqkg^{-1}$) and the gamma dose-rate (i.e. 97.56 $nGyh^{-1}$). This means that the risk associated with exposure to ionizing radiation is high for this location. The mean values of the AEDE is 0.06 $mSvy^{-1}$, which is within the recommended threshold value of 0.07 $mSvy^{-1}$ provided by UNSCEAR (UNSCEAR, 2000). The estimated radium equivalent (Ra_{eq}), H_{ext}, H_{in} and the representative level index (I_γ) follow similar trends with maximum values observed around AG40 as well and minimum values recorded at AG1 respectively. The estimated values for the *ELCR* corroborated our earlier findings with Agbara Bustop 2 and Milo areas recording the maximum and minimum values respectively. The mean values estimated for all the hazard indices are within their corresponding recommended values except for seven locations with values above the average limited given by UNSCEAR (UNSCEAR, 2000). The observed high values at the this location indicates evidence of elevated level of the activity concentrations, which may be attributed to anthropogenic activities going on these areas, and therefore calls for concern. Considerable increase

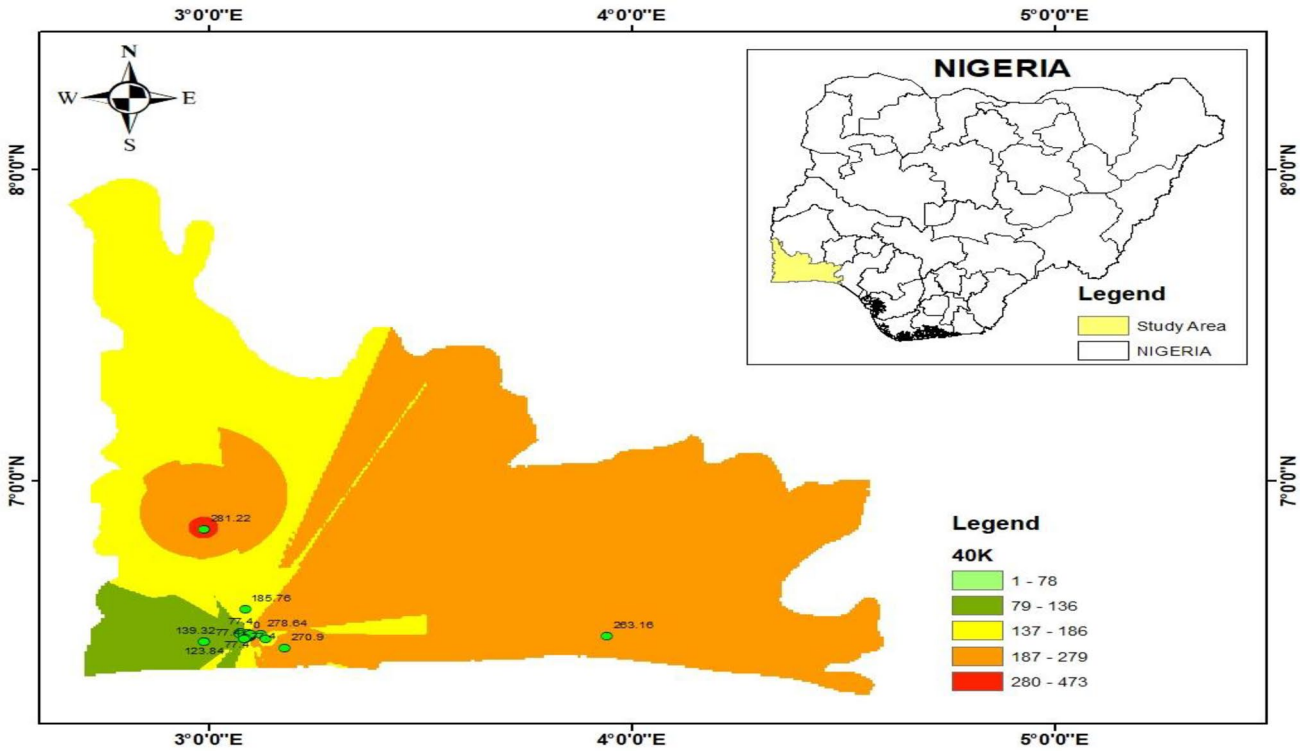

Fig. 2 Spatial distribution of the in-situ measured activity concentration of ^{40}K. Source: authors' computations

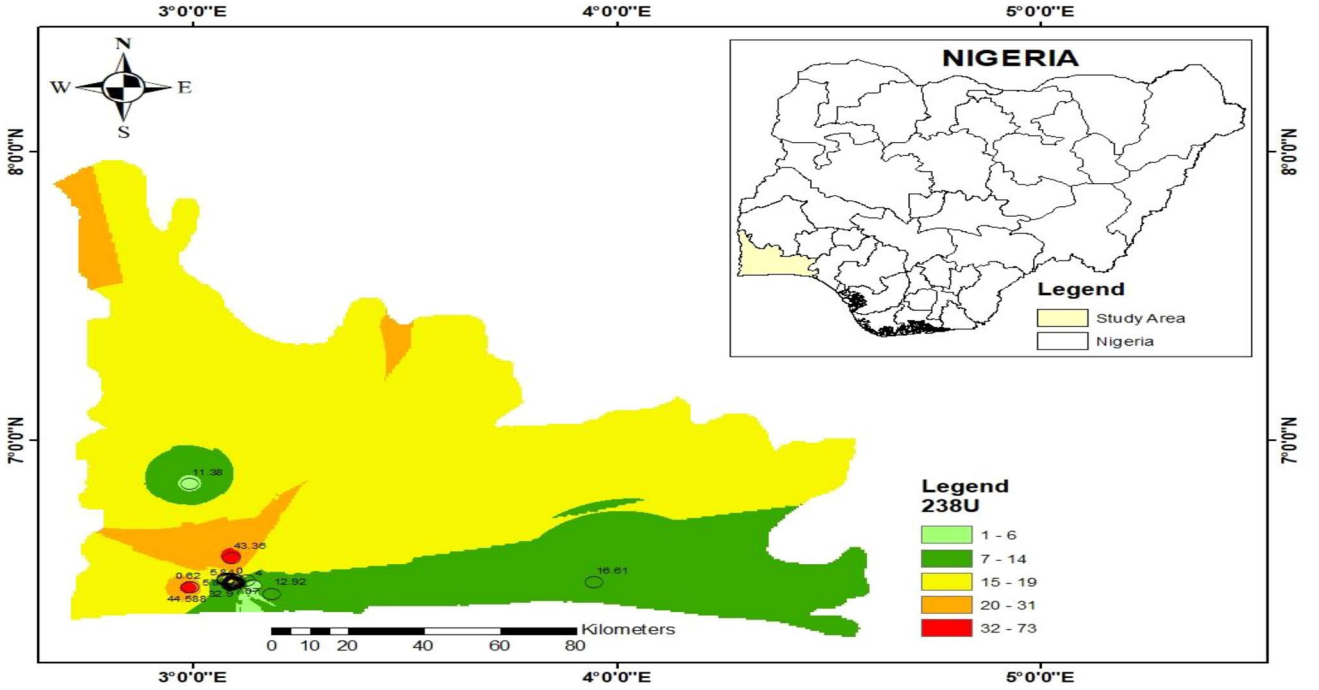

Fig. 3 Spatial distribution of the in-situ measured activity concentration of ^{238}U. Source: authors' computations

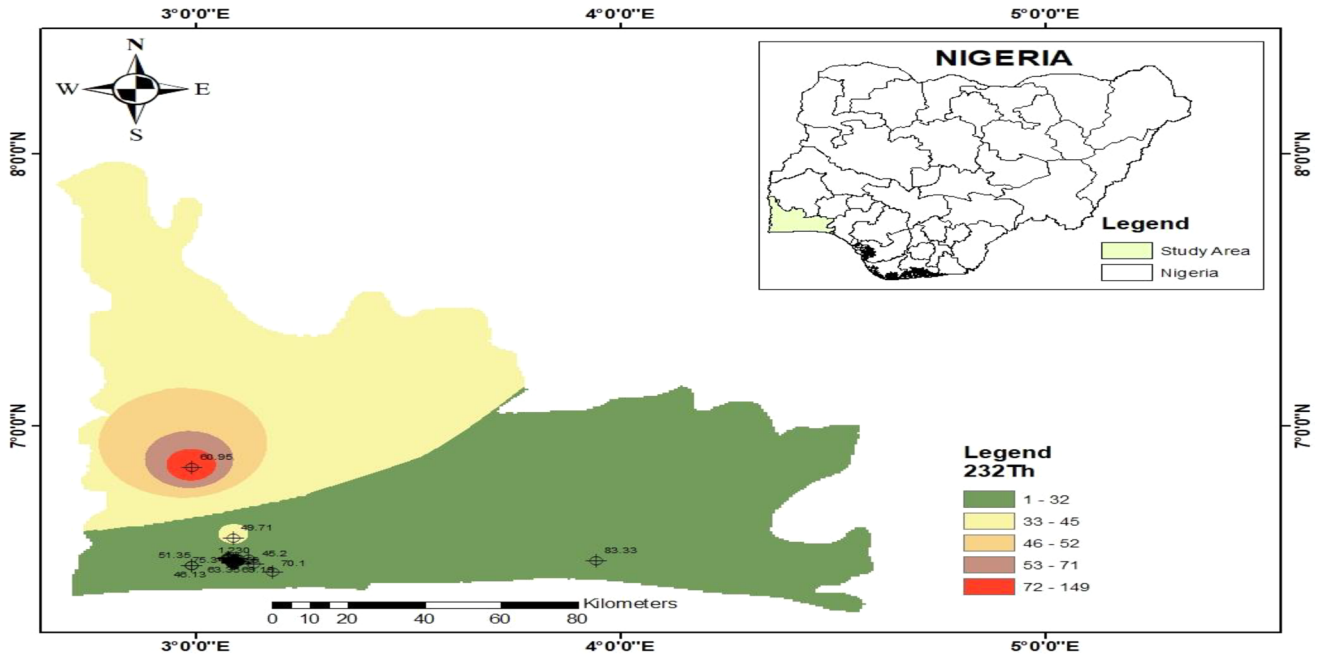

Fig. 4 Spatial distribution of the in-situ measured activity concentration of ^{232}Th. Source: authors' computations

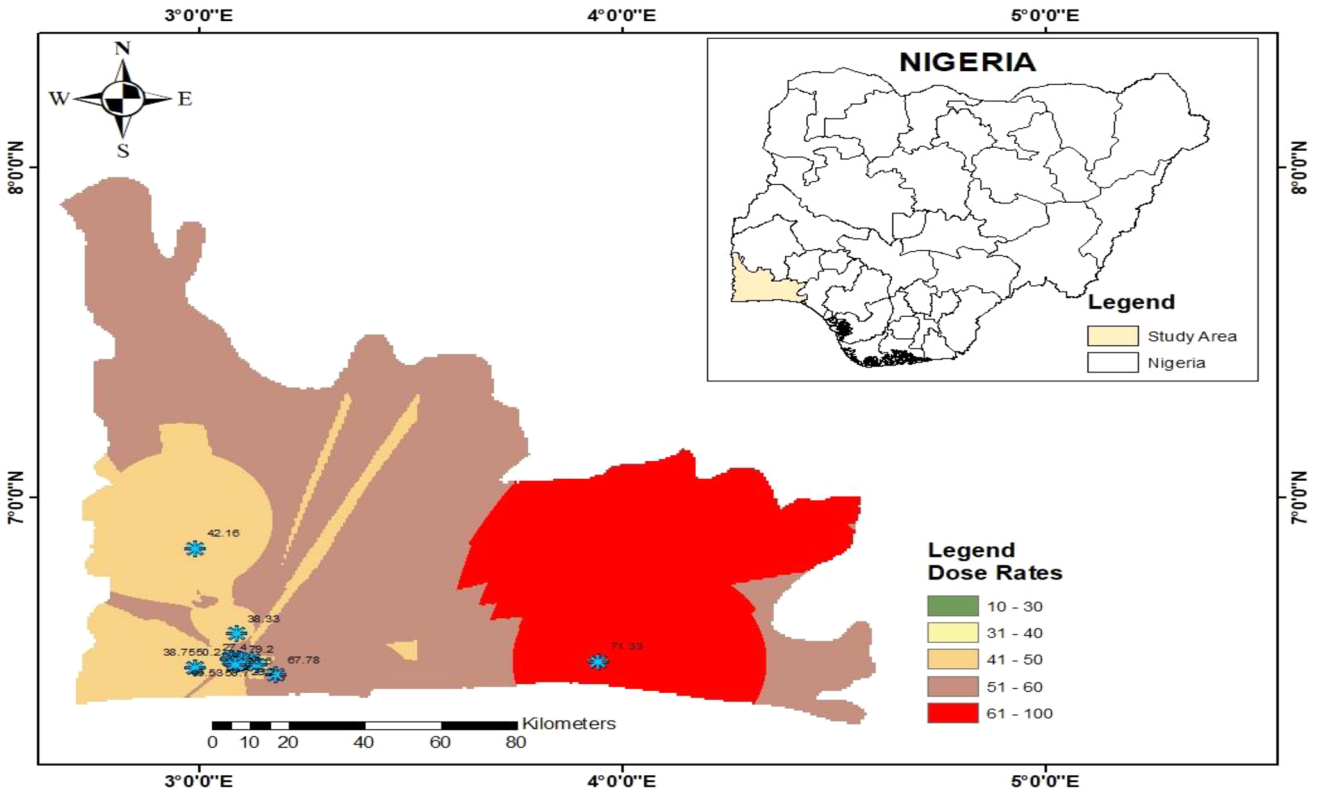

Fig. 5 Spatial distribution of the in-situ measured gamma dose rate (DR). Source: authors' computations

Table 3 Pearson correlation for the primordial radionuclides (^{40}K, ^{238}U, ^{232}Th and the gamma dose-rate (DR))

	DR (nGyh^{-1})	^{40}K (Bqkg^{-1})	^{238}U (Bqkg^{-1})	^{232}Th (Bqkg^{-1})
DR (nGyh^{-1})	1.00			
^{40}K (Bqkg^{-1})	0.50	1.00		
^{238}U (Bqkg^{-1})	0.30	-0.02	1.00	
^{232}Th (Bqkg^{-1})	0.60	0.57	-0.12	1.00

in the concentration of the radionuclides will results in an increase in the level of the background radiation that can lead to exposure to elevated ionization radiation levels. It follows that the Agbara bus stop poses more radiological risks than all the other locations.

Table 4 In-situ radiological hazard indices for the selected locations

S/*N*	Location	Ra_{eq} ($Bqkg^{-1}$)	H_{ex}	H_{in}	D_{out} ($nGyh^{-1}$)	AEDE ($mSvy^{-1)}$	Iγ	ECLR ($x\ 10^{-3}$)
1	AG1	29.19	0.08	0.15	13.42	0.02	0.10	0.06
2	AG2	66.22	0.18	0.26	29.60	0.04	0.23	0.13
3	AG3	141.52	0.38	0.43	61.73	0.08	0.50	0.27
4	AG4	79.18	0.21	0.25	34.71	0.04	0.28	0.15
5	AG5	91.99	0.25	0.26	41.76	0.05	0.34	0.18
6	AG6	120.09	0.32	0.44	53.61	0.07	0.42	0.23
7	AG7	196.66	0.53	0.73	88.59	0.11	0.69	0.38
8	AG8	109.17	0.29	0.35	49.75	0.06	0.40	0.21
9	AG9	99.58	0.27	0.35	43.97	0.05	0.35	0.19
10	AG10	58.75	0.16	0.16	27.62	0.03	0.22	0.12
11	AG11	160.93	0.43	0.52	72.93	0.09	0.58	0.31
12	AG12	60.95	0.16	0.20	26.97	0.03	0.22	0.12
13	AG13	84.78	0.23	0.23	37.10	0.05	0.31	0.16
14	AG14	71.66	0.19	0.26	31.99	0.04	0.25	0.14
15	AG15	106.93	0.29	0.32	48.22	0.06	0.39	0.21
16	AG16	126.28	0.34	0.37	55.41	0.07	0.45	0.24
17	AG17	120.19	0.32	0.36	53.77	0.07	0.44	0.23
18	AG18	206.94	0.56	0.72	92.36	0.11	0.73	0.40
19	AG19	134.02	0.36	0.40	59.58	0.07	0.48	0.26
20	AG20	191.62	0.52	0.58	85.07	0.10	0.69	0.37
21	AG21	128.75	0.35	0.46	57.78	0.07	0.46	0.25
22	AG22	116.73	0.32	0.37	51.96	0.06	0.42	0.22
23	AG23	45.51	0.12	0.25	21.03	0.03	0.15	0.09
24	AG24	98.43	0.27	0.36	44.75	0.05	0.35	0.19
25	AG25	71.65	0.19	0.23	32.08	0.04	0.26	0.14
26	AG26	79.07	0.21	0.22	34.78	0.04	0.28	0.15
27	AG27	64.50	0.17	0.20	28.59	0.04	0.23	0.12
28	AG28	50.96	0.14	0.15	22.20	0.03	0.18	0.10
29	AG29	100.35	0.27	0.32	44.89	0.06	0.36	0.19
30	AG30	156.04	0.42	0.47	68.95	0.08	0.56	0.30
31	AG31	205.38	0.55	0.55	91.03	0.11	0.75	0.39
32	AG32	90.60	0.24	0.29	40.63	0.05	0.33	0.17
33	AG33	73.82	0.20	0.25	32.46	0.04	0.26	0.14
34	AG34	73.62	0.20	0.26	32.28	0.04	0.26	0.14
35	AG35	62.71	0.17	0.21	27.42	0.03	0.22	0.12
36	AG36	124.30	0.34	0.35	54.00	0.07	0.44	0.23
37	AG37	106.62	0.29	0.29	46.92	0.06	0.39	0.20
38	AG38	121.57	0.33	0.41	54.14	0.07	0.43	0.23
39	AG39	119.12	0.32	0.34	52.14	0.06	0.43	0.22
40	AG40	227.61	0.61	0.63	97.56	0.12	0.80	0.42
	LIMITS (UNSCEAR, 2000)	370.00	≤1	≤1	59.00	0.07	≤1	0.29

Table 5 Descriptive statistics of the in-situ radiological hazard indices for the selected locations

Stat	Ra_{eq} ($Bqkg^{-1}$)	H_{ex}	H_{in}	D_{out} ($nGyh^{-1}$)	AEDE ($mSvy^{-1)}$	Iγ	ECLR ($x\ 10^{-3}$)
Minimum	29.19	0.08	0.15	13.42	0.02	0.10	0.06
Maximum	227.61	0.61	0.73	97.56	0.12	0.80	0.42
Mean	109.35	0.30	0.35	48.59	0.06	0.39	0.21
Standard Error	7.54	0.02	0.02	3.32	0.00	0.03	0.01
Median	103.49	0.28	0.33	45.91	0.06	0.37	0.20
Standard Deviation	47.68	0.13	0.15	20.99	0.03	0.17	0.09
Sample Variance	2273.32	0.02	0.02	440.44	0.00	0.03	0.01
Kurtosis	0.18	0.18	0.70	0.06	0.06	0.11	0.06
Skewness	0.80	0.80	1.03	0.78	0.78	0.76	0.78

4 Conclusion

Monitoring of environmental radioactivity due to naturally occurring radionuclides ^{40}K, ^{238}U, and ^{232}Th around Agbara Industrial Area in Ogun, Nigeria, was carried out using RS125 Gamma Spectrometer (a portable NaI [Tl] detector) to detect the level of radiation risks in the areas due to intense anthropogenic activities in the areas. The mean activity concentration of the primordial radionuclides were 177.87 $Bqkg^{-1}$, 20.01 $Bqkg^{-1}$ and 52.90 $Bqkg^{-1}$ for ^{40}K, ^{238}U and ^{232}Th respectively. The in-situ measured dose rate (DR) ranges between 12.18 $nGyh^{-1}$ (Access Bank area) and 97.95 $nGyh^{-1}$ (Market area), with an average value of 47.22 $nGyh^{-1}$. The study revealed that the study locations are rich in thorium as over 50% of study area have ^{232}Th concentration above the world average. Some locations have absorbed dose higher than the recommended limit but the mean measured and estimated absorbed dose rates were within the safe limit of 57 $nGyh^{-1}$ provided by UNSCEAR. The mean values of all the estimated radiological parameters were within the recommended threshold values. It could be concluded that the risk of exposure to higher level of ionizing radiation is low for some locations in Agbara industrial area of Ogun State, but there is a risk of cancer for an individual who has lived in the area for 70 years or more because the excess lifetime cancer risk (ELCR) mean and standard deviation ($0.21 \times 10^{-3} \pm 0.09$) estimated was significantly higher than the UNSCEAR recommended threshold.

Acknowledgements The authors would like to thank the Management of Covenant University for financial support of this present study.

Author Contributions M.R.U designed the research work and edited the final manuscript, A.A, I.O.B, T.E.A. collected samples and data, M.M.O performs the analysis, compiled the work and wrote the original draft, and U.M.A plotted the maps.

Funding The research received funding from Seed Grant from Covenant University Centre for Research Innovation and Discovery.

Data Availability All the data and materials are available.

Declarations

Ethics Approval and Consent to Participate Not applicable (No human or animal specimens are involved).

Consent to Participate All the authors consented to participate.

Consent for Publication All the authors consented and approve the publication of the manuscript.

Competing Interests The authors declare that they have no conflict of interest.

References

Adagunodo T. A, Hammed O. S., Usikalu M. R, Ayara W. A, Ravisankar R. (2018) Data sets on the radiometric survey over a Kaolinitic Terrain in Dahomey Basin, Nigeria. Data Brief 2018(18):814–822

Adagunodo TA, Sunmonu LA, Adabanija MA, Omeje M, Odetunmibi OA, Ijeh V (2019) Statistical assessment of radiation exposure risks to farmers in Odo Oba, South Western Nigeria. Bull Min Res Exp 159:201–217. https://doi.org/10.19111/bulletinofmre.495321

Ademola AK, Bello AK, Adejumobi AC (2014) Determination of natural radioactivity and hazard in soil samples in and around gold mining area in Itagunmodi, south-western, Nigeria. J Radiation Res Appl Sci 7(3):249–255

Ajibola TB, Orosun MM, Ehinlafa OE, Sharafudeen FA, Salawu BN, Ige SO, Akoshile CO (2022) Radiological hazards Associated with 238U, 232Th, and 40K in some selected packaged drinking Water in Ilorin and Ogbomoso, Nigeria. Pollution 8(1):117–131. https://doi.org/10.22059/poll.2021.325859.1119

IAEA (1989) International Atomic Energy Agency: Construction and Use of Calibration Facilities for Radiometric Field Equipment. Technical Reports Series No. 309, IAEA, Vienna, 1989

IAEA (1996) International Atomic Energy Agency: Radiation protection and the safety of Radiation sources, A1400 Vienna, Austria. IAEA-RPSR-1 Rev 1

ICRP (1991) Recommendations of the International Commission on Radiological Protection 1990 (ICRP) publication 60. Ann ICRP 21:1–201

Omeje M, Olusegun OA, Joel ES et al (2021) Measurements of Seasonal variations if Radioactivity distributions in Riverine Soil Sediment of Ado-Odo Ota, South-West Nigeria: Probabilistic Approach using Monte Carlo. Radiat Prot Dosimetry 193(2):76–89. https://doi.org/10.1093/rpd/ncab027

Omeje M, Orosun MM, Adewoyin OO et al (2022) Radiotoxicity Risk Assessments of ceramic tiles used in Nigeria: The Monte Carlo Approach. Environmental Nanotechnology, Monitoring & Management. 100618. https://doi.org/10.1016/j.enmm.2021.100618

Omeje M, Aimua GU, Adewoyin OO et al (2023) Dispersion of gamma dose rates and natural radionuclides in the coastal environments of the unumherin community in Niger Delta. Cogent Eng 10:1. https://doi.org/10.1080/23311916.2023.2204546

Omeje M, Orosun MM, Aimua GU et al (2024) Radioactivity distributions and biohazard assessment of coastal marine environments of Niger-Delta. Nigeria All Earth 36(1):1–19. https://doi.org/10.1080/27669645.2023.2299109

Orosun MM, Lawal TO, Ezike SC, Salawu NB, Atolagbe BM, Akinyose FC, Ige SO, Martins G (2017) Natural radionuclide concentration and radiological impact assessment of soil and water from Dadinkowa Dam, Northeast Nigeria. J Nigerian Association Math Phys 42(1):307–316

Orosun MM, Usikalu MR, Oyewumi KJ, Adagunodo AT (2019) Natural radionuclides and Radiological Risk Assessment of Granite Mining Field in Asa, North-central Nigeria. MethodsX 6:2504–2514. https://doi.org/10.1016/j.mex.2019.10.032

Orosun MM, Usikalu MR, Kayode KJ (2020) Radiological hazards assessment of laterite mining field in Ilorin, North-central Nigeria. Int J Radiation Res 18(4):895–906

Orosun MM, Ajibola TB, Farayade BR, Akinyose FC, Salawu NB, Louis H, Ajulo KR, Adewuyi AD (2021) Radiological impact of mining: new insight from cancer risk assessment of radon in water from Ifelodun beryllium mining, North-Central Nigeria using Monte Carlo simulation. Arab J Geosci 14:2380. https://doi.org/10.1007/s12517-021-08670-3

Orosun MM, Usikalu MR, Oyewumi KJ, Omeje M, Awolola GV, Ajibola O, Tibbett M (2022a) Soil-to-plant transfer of ^{40}K, ^{238}U and ^{232}Th and radiological risk assessment of selected mining sites in Nigeria. Heliyon 8(11):e11534. https://doi.org/10.1016/j.heliyon.2022.e11534

Orosun MM, Usikalu MR, Oyewumi KJ, Onumejor CA, Ajibola TB, Valipour M, Tibbett M (2022b) Environmental Risks Assessment of Kaolin Mines and their Brick products using Monte Carlo simulations. Earth Syst Environ 6:157–174. https://doi.org/10.1007/s41748-021-00266-x

Oyeyemi KD, Usikalu MR, Aizebeokhai AP, Achuka JA, Jonathan O (2017) Measurements of radioactivity levels in part of Ota Southwestern Nigeria: Implications for radiological hazards indices and excess lifetime cancer-risks. Journal of Physics: IOP Conference Series 852: 012042

UNSCEAR, United Nations Scientific Committee on the Effects of Atomic Radiation Sources, effects and risks of ionization radiation (2000) Report Vol 1 to the General Assembly, with scientific annexes. New York: United Nations, Sales Publications; 2000. https://doi.org/10.18356/49c437f9-en

UNSCEAR, United Nations Scientific Committee on Effect of Atomic Radiation Sources and Effect of Ionising Radiation (2008). Report Vol. 1 to the General Assembly with scientific Annexes. New York: United Nations, Sales Publications; 2008. https://doi.org/10.18356/9b8f628f-en

Usikalu MR, Maleka PP, Malik M, Oyeyemi KD, Adewoyin OO (2016) Assessment of geogenic natural radionuclide contents of soil samples collected from Ogun State, South Western, Nigeria. Int J Radiation Res 14(3):355–361

Usikalu MR, Fuwape IA, Jatto SS, Awe OF, Rabiu AB, Achuka JA (2017) Assessment of radiological parameters of soil in Kogi State, Nigeria. Environ Forensics 18(1):1–14. https://doi.org/10.1080/15275922.2016.1263898

Usikalu MR, Morakinyo RO, Enemuwe CA, Orosun MM, Adagunodo TA, Achuka JA (2020) Background Radiation from ^{238}U, ^{232}Th, and ^{40}K in bells Area and Canaan City, Ota, Nigeria. Open Access Maced. J Med Sci 8(E):678–684. https://doi.org/10.3889/oamjms.2020.5434

Usikalu MR, Morakinyo RO, Orosun MM, Achuka JA (2023) Assessment of background Radiation in Ojota Chemical Market, Lagos, Nigeria. J Hazard Toxic Radioactive Waste 27(1):04022041. https://doi.org/10.1061/(ASCE)HZ.2153-5515.0000732